Journal of Alloys and Compounds 486 (2009) 246–249

Contents lists available at ScienceDirect

Journal of Alloys and Compounds

journal homepage: www.elsevier.com/locate/jallcom

Review

# Formation and properties of $Ba_xFe_{3-x}O_4$ with spinel structure by mechanochemical reaction of $\alpha$-$Fe_2O_3$ and $BaCO_3$

Q. He [a], H.Z. Wang [a], G.H. Wen [c], Y. Sun [a], B. Yao [a,b,*]

[a] Department of Physics, Jilin University, Changchun 130021, People's Republic of China
[b] Laboratory of Excited State Processes, Changchun Institute of Optics, Fine Mechanics and Physics, Chinese Academy of Sciences, Changchun 130021, People's Republic of China
[c] State Key Laboratory of Superhard Materials, Jilin University, Changchun 130012, People's Republic of China

ARTICLE INFO

*Article history:*
Received 15 April 2009
Received in revised form 19 June 2009
Accepted 22 June 2009
Available online 30 June 2009

*Keywords:*
Spinel structure
Mechanochemical reaction
X-ray diffraction analysis
VSM measurement

ABSTRACT

Magnetic $Ba_xFe_{3-x}O_4$ ($x \sim 0.23$) with spinel structure was fabricated by ball milling of mixture of $BaCO_3$ and nonmagnetic $\alpha$-$Fe_2O_3$ powders, and the molar ratio of $BaCO_3$ and $\alpha$-$Fe_2O_3$ is 1:6. In the milling process, a mechanochemical reaction took place between $BaCO_3$ and $\alpha$-$Fe_2O_3$, and Ba cation incorporated into $\alpha$-$Fe_2O_3$ with rhombohedral structure to form a $\alpha$-$(Fe,Ba)_2O_3$ solid solution. The Ba content in the $\alpha$-$(Fe,Ba)_2O_3$ increased with increasing milling time, when the Ba content exceeded a limited solubility, the $\alpha$-$(Fe,Ba)_2O_3$ transformed into a phase of $Ba_xFe_{3-x}O_4$ with spinel structure, where the Ba cation occupied an octahedral site or tetrahedral site. The product obtained in the balling process was different from that prepared in the annealing process at atmospheric pressure, which was $BaFe_2O_4$ with orthorhombic structure. Accompanying the crystal structure transition from $\alpha$-$(Fe,Ba)_2O_3$ to $Ba_xFe_{3-x}O_4$, the magnetic properties also changed from nonmagnetism into ferromagnetism. The saturation magnetization was 53.3 emu/g and coercivity was 113.7 Oe. The mechanism of transitions of the crystal structure was discussed in the present work.



**Contents**



## 1. Introduction

The development of ferrite materials, such as, $\alpha$-$Fe_2O_3$ (hematite), $\gamma$-$Fe_2O_3$ (maghemite) and $Fe_3O_4$ (magnetite), has attracted much attention of researchers for a long time, due to their important application in electrical and magnetic devices. Especially, $Fe_3O_4$ with spinel structure belongs to a kind of soft magnetic materials, and is widely used in radio frequency (RF) and microwave (MW), etc. devices. In the recent years, many attempts have been done to incorporate an element into ferrite to obtain a new kind of tri-element ferrites or improve properties of ferrites. For example, the spinel type $M_xFe_{3-x}O_4$ is of great value in the view of ferrofluid, magnetic drug delivery, magnetic recording media, etc. [1–3].

In order to improve physical and chemical properties of ferrite and fabricate of new ferrite, cation substitution in spinels may be at one or both cation sites, with magnetic or nonmagnetic ions with different valence [4]. Cations incorporated in spinel lattice change magnetic interactions and magnetic anisotropy, influencing the saturation magnetization and coercivity values of parent compounds [5] such as, Ni, Zn [6,7], Ho [8], Li [9], Mg [10,11] and so on. Ba element is recently considered as a good candidate for changing magnetic properties of ferrite recently, for example, it makes the soft magnetic or nonmagnetic ferrite change into hard magnetic barium ferrite.

It is well known that physical and chemical properties of a material depend on its crystal structure, which is usually influenced by

* Corresponding author at: Department of Physics, Jilin University, Jiefang Road 2519, Changchun, 130021, People's Republic of China. Tel.: +86 431 86176355; fax: +86 431 86176288.
*E-mail address:* binyao@jlu.edu.cn (B. Yao).

0925-8388/$ – see front matter © 2009 Elsevier B.V. All rights reserved.
doi:10.1016/j.jallcom.2009.06.142

the preparation methods and conditions. High-energy ball milling technique has attracted much attention in the materials science field. It has been used in the preparation of alloy, amorphous alloy, nanostructured materials and other new matters, and is considered as an effective technique to fabricate new kind of materials, especially those materials which cannot be produced in thermodynamic equilibrium state, such as non-miscible materials [12,13]. Recently, mechanochemical processing activated by high-energy ball milling has been successfully used to prepare high quality ferrite nanoparticles [14,15].

In the present work, the ball milling technique is used to prepare new kind of ferrite containing Ba, and a particular $Ba_xFe_{3-x}O_4$ with spinel structure is synthesized by using mechanochemical reaction of $\alpha$-$Fe_2O_3$ and $BaCO_3$. Its formation mechanism and properties are discussed.

## 2. Experimental procedures

A mixture of 99% pure nonmagnetic $\alpha$-$Fe_2O_3$ and $BaCO_3$ powders were used as starting materials for production of $Ba_xFe_{3-x}O_4$ by mechanochemical reaction in a high-energy ball mill. The molar ratio of $\alpha$-$Fe_2O_3$ to $BaCO_3$ was 6:1 in the mixture. A stainless vial filled with stainless balls having diameter of 5–15 mm was used as the milling medium. The mass of the powder was 7 g and the balls-to-powder mass ratio was 15:1. The mixture was milled under air ambient without any additive (dry milling). In order to investigate the forming process of the $Ba_xFe_{3-x}O_4$, the mechanical milling was interrupted every 5 h to take a small amount of samples from the vial for various analyses. The mixture was also pressed into disk and sintered for 2 h in air atmosphere in a temperature ranging from 300 to 1000 °C to compare the reaction between $\alpha$-$Fe_2O_3$ and $BaCO_3$ in the sintering process with that of in the ball milling process.

The structure of the samples were characterized by using a Rigaku-D-Max X-ray diffractometer (XRD) with Cu K$\alpha$ radiation ($\lambda$ = 1.5418 Å). Composition of the sample was detected by energy dispersive X-ray spectroscopy (EDS) microanalysis equipped in a scanning electron microscopy (SEM) (JEOL JXA-8200) and X-ray photoelectron spectrometry (XPS) (Thermo ECSAlAB250) with Al K$\alpha$ X-ray source. The binding energy scale was calibrated by C1s peak of 284.55 eV. Magnetic measurement was performed in a vibrating sample magnetometer (VSM) at room temperature with a maximum applied field of 1100 kA/m. (Lake Shore 7410 vibrating sample magnetometer)

## 3. Results and discussion

Fig. 1(a)–(d) shows XRD patterns of the mixture of the $\alpha$-$Fe_2O_3$ (hematite) and $BaCO_3$ milled for 0, 10, 40 and 80 h, respectively. Fig. 1(a) indicates that the starting mixture consists of $\alpha$-$Fe_2O_3$ and $BaCO_3$. Upon milling of 10 h, the diffraction peaks intensity of the $BaCO_3$ decrease greatly and the diffraction peak positions of $\alpha$-$Fe_2O_3$ shift towards low diffraction angle, as shown in Fig. 1(b). Since atomic radius of Ba is larger than that of Fe, the decrease in diffraction angle is due to the fact that some Ba cations have substituted for Fe cations in the $\alpha$-$Fe_2O_3$ to form $\alpha$-$(Fe,Ba)_2O_3$ solid solution.

When extending milling time to 40 h, as Fig. 1(c) shows, two additional weak diffraction peaks, located at 29.98° and 42.82°, respectively, were observed besides diffraction peaks of $\alpha$-$(Fe,Ba)_2O_3$ solid solution. The *d* values of the peaks at 29.98° and 42.82° are close to the *d* values of (2 2 0) and (4 0 0) plane of $Fe_3O_4$ with spinel structure, respectively. So, we deduced that some $\alpha$-$(Fe,Ba)_2O_3$ transform into Ba-containing $Fe_3O_4$ solid solution.

Fig. 1(d) shows XRD pattern of the mixture milled for 80 h, indicating that the diffraction peaks of the $\alpha$-$(Fe,Ba)_2O_3$ almost disappear, instead some strong diffraction peaks, located at 18.31°, 30.16°, 35.49°, 43.10°, 53.46°, 57.00°, 62.59° and 74.24°, respectively, appear. The *d* values of these peaks are close to that of $Fe_3O_4$ with spinel structure, and the ratio of square of reciprocal of the *d* values is 3:4:8:11:..., which is a characteristic of face-centered cubic structure, indicating that the phase related to these diffraction peaks is of spinel structure. Based on the discussion mentioned above, it is concluded that the most of $\alpha$-$(Fe,Ba)_2O_3$ transform into of Ba–Fe–O phase with spinel structure (denoted as $Ba_xFe_{3-x}O_4$ in the following) upon milling of 80 h. Only a little of $\alpha$-$(Fe,Ba)_2O_3$ remained.

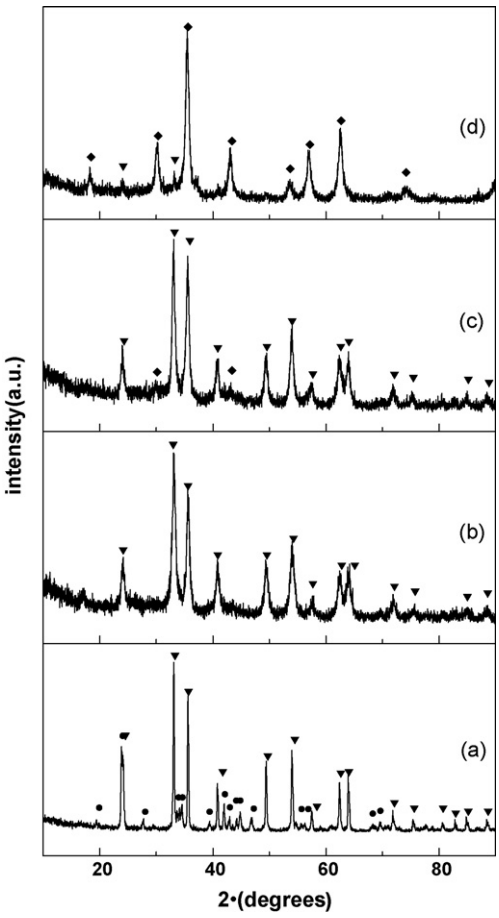


**Fig. 1.** XRD pattern of the mixture of $\alpha$-$Fe_2O_3$ and $BaCO_3$ powder milled for 0 h (a), 10 h (b), 40 h (c), 80 h (d): (▼) $\alpha$-$Fe_2O_3$; (●) $BaCO_3$; (♦) $Ba_xFe_{3-x}O_4$.

By using XRD results of Fig. 1, lattice constants of $\alpha$-$Fe_2O_3$ as well as $\alpha$-$(Fe,Ba)_2O_3$ and $Ba_xFe_{3-x}O_4$ prepared at various milling time are calculated, as shown in Fig. 2. It can be seen from Fig. 2 that the lattice constant of $\alpha$-$Fe_2O_3$ in *a*-axis is *a* = 0.5038 nm and

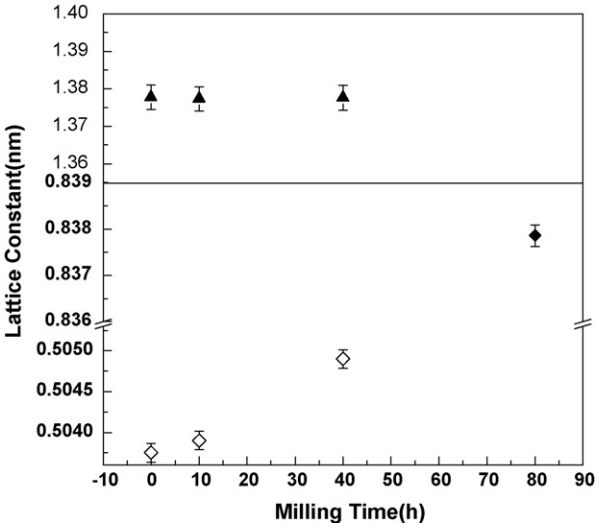


**Fig. 2.** Plot of lattice constant *a* (a) and *c* (b) of $\alpha$-$Fe_2O_3$ milled for 0, 10 and 40 h and $Ba_xFe_{3-x}O_4$ (◊) lattice constant *a* of $\alpha$-$Fe_2O_3$; (♦) lattice constant *a* of $Ba_xFe_{3-x}O_4$; (▲) lattice constant *c* of $\alpha$-$Fe_2O_3$.

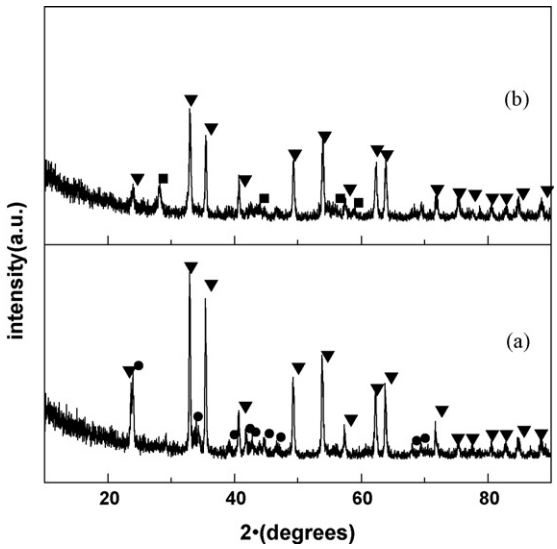


**Fig. 3.** XRD pattern of the mixture of α-$Fe_2O_3$ and $BaCO_3$ powder sintered for 400 °C (a) and 700 °C (b), respectively: (▼) α-$Fe_2O_3$; (●) $BaCO_3$; (■) $BaFe_2O_4$.

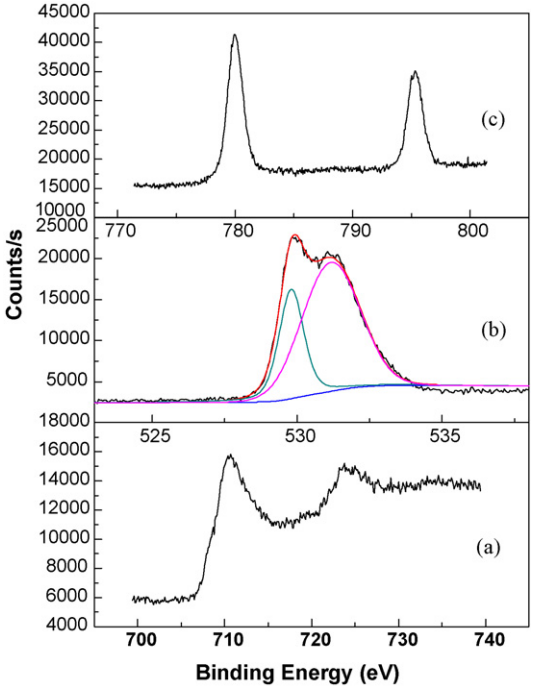


**Fig. 4.** XPS spectrum of O1s (a), Fe2p (b) and Ba (c) of the $Ba_xFe_{3-x}O_4$.

increases with increasing milling time due to incorporation of Ba into the α-$Fe_2O_3$ to form α-$(Fe,Ba)_2O_3$ solid solution. Upon milling 40 h, this value reaches 0.5049 nm, but the constant in *c*-axis almost does not change with milling time, as shown in Fig. 2(b). However, as milling time reaches 80 h, almost all of α-$(Fe,Ba)_2O_3$ transform into $Ba_xFe_{3-x}O_4$, implying that there is a limited solubility for incorporation of Ba into α-$Fe_2O_3$ and when the concentration of Ba in α-$(Fe,Ba)_2O_3$ exceeds the limited solubility, α-$(Fe,Ba)_2O_3$ transforms into $Ba_xFe_{3-x}O_4$. The lattice constant of the $Ba_xFe_{3-x}O_4$ is measured to be 0.8381 nm. The $Ba_xFe_{3-x}O_4$ has similar structure to $Fe_3O_4$ implying that it is a Ba cation substitute for Fe cation of oxide.

In order to understand the effect of Ba on formation of the $Ba_xFe_{3-x}O_4$, 99% pure α-$Fe_2O_3$ powder was milled up to 80 h, but no change in structure was observed. This indicates that the incorporation of Ba into α-$Fe_2O_3$ has important role for formation of the $Ba_xFe_{3-x}O_4$.

A mixture of α-$Fe_2O_3$ and $BaCO_3$ with the same molar ratio as that of ball milling process was sintered for 2 h at 400 and 700 °C, respectively in order to explain effect of ball milling on the formation of the $Ba_xFe_{3-x}O_4$. Fig. 3(a) shows XRD pattern of mixture of α-$Fe_2O_3$ and $BaCO_3$ sintered at 400 °C, indicating that no reaction occurs between α-$Fe_2O_3$ and $BaCO_3$. However, when the mixture was sintered at 700 °C, it is found that diffraction peaks intensity of $BaCO_3$ decrease greatly, as shown in Fig. 3(b). At the same time, some additional diffraction peaks were observed in the XRD profile besides diffraction peaks of α-$Fe_2O_3$. These additional peaks are attributed to the diffractions of $BaFe_2O_4$ with orthorhombic structure. This implies that the α-$Fe_2O_3$ reacts with $BaCO_3$ to form $BaFe_2O_4$ with orthorhombic structure as they are sintered at 700 °C in ambient air, in agreement with literature reported previously [16] where the reaction occurs at temperatures of 600–750 °C and can be expressed as:

$$BaCO_3 + Fe_2O_3 \rightarrow BaFe_2O_4 + CO_2$$

Based on the above discussion, it can be concluded that the reaction between α-$Fe_2O_3$ and $BaCO_3$ cannot form the $Ba_xFe_{3-x}O_4$ with spinel structure but $BaFe_2O_4$ with orthorhombic structure, if they are sintered in air ambient.

The difference in the reaction product of α-$Fe_2O_3$ and $BaCO_3$ in sintering and ball milling processes implies the two processes have different reaction mechanisms. The reaction is performed in thermodynamic equilibrium state for a sintering process, but in thermodynamic non-equilibrium state for a ball milling process. In sintering process the reaction between α-$Fe_2O_3$ and $BaCO_3$ is affected by temperature, whereas in ball milling process local pressure and local temperature induced by collision between balls or balls and vial play a major role [17]. The local pressure is about 3–5 GPa, and the local temperature is in a range of 300–500 °C [18]. It is reported previously that the local pressure and local temperature have important influence on a chemical reaction process, resulting in formation of particular phases which usually cannot be obtained in thermodynamic equilibrium process at atmospheric pressure [19]. In fact, when α-$Fe_2O_3$ and $BaCO_3$ are refined in grain size in the ball milling process, at the same time they are also contacted tightly to form a α-$Fe_2O_3$/$BaCO_3$ interfaces due to repeated impacting between them. The grain size refinement enhances reaction activation, while the interface formation reduces diffusion distances. In addition, catalysis of α-$Fe_2O_3$ also decreases decomposition temperature of $BaCO_3$ [20]. The three factors make chemical reaction temperature between α-$Fe_2O_3$ and $BaCO_3$ decrease, and the reaction can occur at the local temperature, smaller than the reaction temperature of 700 °C in the sintering process.

Since ball milling is a thermodynamic non-equilibrium process, some Ba can incorporate into α-$Fe_2O_3$ by diffusion reaction between α-$Fe_2O_3$ and $BaCO_3$ at their interface, and form α-$(Fe,Ba)_2O_3$ driven by local temperature, which are not obtained in thermodynamic equilibrium process. With increasing milling time, Ba content in α-$(Fe,Ba)_2O_3$ increases. When it exceeds the limited solubility of Ba in the α-$(Fe,Ba)_2O_3$, the α-$(Fe,Ba)_2O_3$ will undergo phase transition.

In order to investigate the chemical composition and valence state of the $Ba_xFe_{3-x}O_4$, XPS measurement is performed, as shown in Fig. 4(a–c). Fig. 4(a) shows two peaks, located at 710.49 and 723.60 eV, respectively, which are due to $Fe_{2p3/2}$ and $Fe_{2p1/2}$ core radiation in $Fe_3O_4$, respectively and characteristics of $Fe^{3+}$ in $Fe_3O_4$ material [21]. The peaks located at 529.80 and 531.17 eV shown in Fig. 4(b) correspond to O1s radiation in $Fe_3O_4$ and adsorbed $OH^-$ material, respectively [22]. Fig. 4(c) shows that the binding energy of barium is 779.96 and 795.30 eV, which are consistent to values of $Ba_{3d5/2}$ and $Ba_{3d3/2}$ in Ba–O bond, respectively, implying that Ba

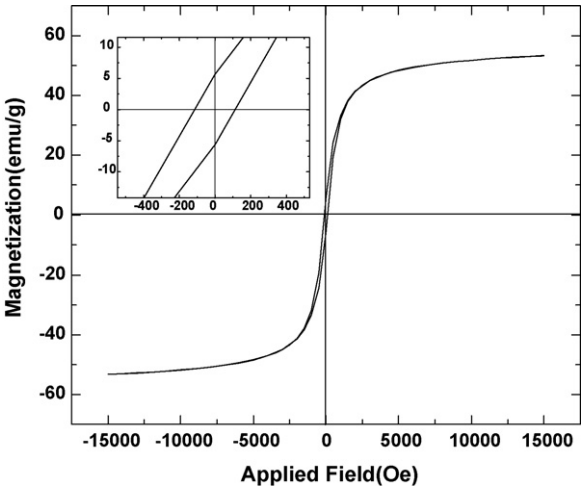


**Fig. 5.** Hysteresis loop of the $Ba_xFe_{3-x}O_4$. The inset is the hysteresis loop in magnetic field ranging from −400 to 400 Oe.

shows valence state of +2 and substitutes for $Fe^{+2}$ when it incorporates into $Fe_3O_4$. EDS measurement indicates that the atomic ratio of Fe to Ba in starting mixture is close to that in the 80-milled mixture, implying that almost all Ba incorporate into $Ba_xFe_{3-x}O_4$. The atomic ratio of Fe/Ba is about 12:1

As it is known, $Fe_3O_4$ has a spinel crystal structure, its unit cell contains 32 oxygen atoms, 8 equivalent tetrahedral and 16 equivalent octahedral sites [23], and the octahedral volume is larger than tetrahedral volume. In the structure of $Fe_3O_4$, the tetrahedral sites are completely occupied by $Fe^{3+}$, the 16 octahedral ones are occupied by equal amounts of $Fe^{3+}$ and $Fe^{2+}$ [24], that is 8 $Fe^{3+}$ and 8 $Fe^{2+}$ ions. In the present work, Ba substitutes for Fe and occupies the tetrahedral or octahedral sites in the spinel structure. The atomic ratio of Ba to Fe is about 1–12 measured by EDS. Since the amount of the α-$(Fe,Ba)_2O_3$ are small, as shown in Fig. 1(d), we neglect the influence of the amount of the α-$(Fe,Ba)_2O_3$. Based on the EDS measurement result, thus the estimated Ba content $x$ in $Ba_xFe_{3-x}O_4$ is found to be about 0.23 and the Fe content is found to be 2.77. As such, the $Ba_xFe_{3-x}O_4$ can be expressed as $Ba_{0.23}Fe_{2.77}O_4$.

The magnetic properties of the sample are measured by VSM at room temperature. Fig. 5 shows the magnetization as a function of applied magnetic field measured at room temperature for the composition that is mechanically activated for 80 h. The hysteresis loop of $Ba_xFe_{3-x}O_4$ powder shows a ferromagnetic behavior with high saturation magnetization of 53.27 emu/g and coercivity of 113.75 Oe. The inset is the hysteresis loop in magnetic field ranging from −400 to 400 Oe, which helps us measure the coercivity exactly. The value of saturation magnetization is slightly lower than value of $Fe_3O_4$ nanoparticles (59 emu/g) [25] but is much lower than that of bulk $Fe_3O_4$ (92 emu/g) [26]. This may be due to the shape anisotropy of nanorods to prevent them from magnetizing in directions other than along their easy magnetic axes.

## 4. Conclusions

A $Ba_{0.23}Fe_{2.77}O_4$ with spinel structure is prepared by ball milling the mixture of α-$Fe_2O_3$ and $BaCO_3$ with molar ratio of 6:1 for 80 h, which is completely different from the result obtained in sintering process at atmospheric pressure, where the reaction product of α-$Fe_2O_3$ and $BaCO_3$ is $BaFe_2O_4$ with orthorhombic structure. In the ball milling process, α-$(Fe,Ba)_2O_3$ solid solution forms firstly by diffusion reaction driven by local temperature, and the Ba content in α-$(Fe,Ba)_2O_3$ increases with increasing milling time; as the Ba content exceeds a limited solubility, the α-$(Fe,Ba)_2O_3$ transforms into $Ba_{0.23}Fe_{2.77}O_4$ with higher density due to effect of local pressure. The formation of $Ba_{0.23}Fe_{2.77}O_4$ is related to the incorporation of Ba into α-$Fe_2O_3$ and the local pressure. Grain size refinement and formation of α-$Fe_2O_3$/$BaCO_3$ interfaces induced by the milling as well as catalysis of α-$Fe_2O_3$ on decomposition of $BaCO_3$ make the chemical reaction occur at lower temperature. The $Ba_{0.23}Fe_{2.77}O_4$ shows ferromagnetic properties with saturation magnetization of 53.3 emu/g and the coercivity of 113.7 Oe.

## Acknowledgements

We would like to thank financial support of Key Projects of the National Natural Science Foundation of China (Grant Nos. 60336020 and 50532050), and the National Natural Science Foundation of China (Grant Nos. 50472003, 60776011, and 10874178).

## References

[1] H.B. Wang, J.H. Liu, W.F. Li, J.B. Wang, L. Wang, L.J. Song, S.J. Yuan, F.S. Li, J. Alloys Compd. 461 (2008) 373–377.
[2] M. Zdujić, C. Jovalekić, Lj. Karanović, M. Mitrić, D. Poleti, D. Skala, Mater. Sci. Eng. A A245 (1998) 109–117.
[3] Z. Cvejic, S. Rakic, A. Kremenovic, B. Anticc, C. Jovalekic, P. Colomban, Solid State Sci. 8 (2006) 908–915.
[4] B. Antic, A. Kremenovic, A.S. Nikolic, M. Stoiljkovic, J. Phys. Chem. B 108 (2004) 12646.
[5] Z. Cvejic, B. Antic, A. Kremenovic, S. Rakic, G.F. Goya, H.R. Rechenberg, C. Jovalekic, V. Spasojevic, J. Alloys Compd. 472 (2009) 571–575.
[6] S.E. Jacobo, S. Duhalde, H.R. Bertorello, J. Magn. Magn. Mater. 272–276 (2004) 2253–2254.
[7] K. Park, J.K. Lee, J. Alloys Compd. 475 (2009) 513–517.
[8] R.V. Upadhyay, A. Gupta, C. Sudakar, K.V. Rao, K. Parekh, R. Desai, R.V. Mehta, J. Appl. Phys. 99 (08) (2006) M906.
[9] J. Jiang, Y.-M. Yang, L.-C. Li, J. Alloys Compd. 464 (2008) 370–373.
[10] H.M. Widatallah, C. Johnson, A.M. Gismelseed, I.A. Al-Omari, S.J. Stewart, S.H. Al-Harthi, S. Thomas, H. Sitepu, J. Phys. D: Appl. Phys. 41 (2008) 165006.
[11] S.M. Yunus, H. Yamauchi, A.K.M. Zakaria, N. Igawa, A. Hoshikawa, Y. Ishii, J. Alloys Compd. 454 (2008) 10–15.
[12] M. Abdellaoui, E. Gaffet, Acta Metall. Mater. 43 (1995) 1087–1098.
[13] Y. Sun, B. Yao, Q. He, F. Su, H.Z. Wang, J. Alloys Compd. 479 (2009) 599–602.
[14] J. Ding, T. Tsuzuki, P.G. McCormick, J. Magn. Magn. Mater. 177–181 (1998) 931–932.
[15] Y. Shi, J. Ding, H. Yin, J. Alloys Compd. 308 (2000) 290–295.
[16] H.P. Steier, J. Requena, J.S. Moya, J. Mater. Res. 14 (1999) 3647–3652.
[17] B. Yao, L. Liu, S.E. Liu, B.Z. Ding, W.H. Su, Y. Li, J. Non-Cryst. Solids 277 (2000) 91–97.
[18] M.L. Trudeau, R. Schulz, D. Dussault, A. Van Neste, Phys. Rev. Lett. 46 (1990) 99–102.
[19] T. Aboud, B.-Z. Weiss, R. Chaim, Nanostruct. Mater. 6 (1995) 405–408.
[20] C.H. Li, W.H. Qiu, X.L. Kang, K.C. Chou, X.G. Lu, F.S. Li, Acta Phys. Chim. Sin. 24 (5) (2008) 767–771.
[21] D.B. Shieh, F.Y. Cheng, C.H. Su, C.S. Yeh, M.T. Wu, Y.N. Wu, C.Y. Tsai, C.L. Wu, D.H. Chen, C.H. Chou, Biomaterials 26 (2005) 7183–7191.
[22] J.L. Zhao, X.H. Wang, L.T. Li, X.X. Wang, Y.X. Li, Ceram. Int. 34 (2008) 1223–1227.
[23] I. Mitov, Z. Cherkezova-Zheleva, V. Mitrov, Phys. Status Solidi A 161 (1997) 475–482.
[24] R. Janot, D. Guerard, Prog. Mater. Sci. 50 (2005) 1–92.
[25] K. Simeonidis, S. Mourdikoudis, I. Tsiaoussis, M. Angelakerisa, C. Dendrinou-Samara, O. Kalogirou, J. Magn. Magn. Mater. 320 (2008) 1631–1638.
[26] D.H. Han, J.P. Wang, H.L. Luo, J. Magn. Magn. Mater. 136 (1994) 176–182.